Springer

Journal of Mechanical Science and Technology 23 (2009) 614~623

Journal of Mechanical Science and Technology

www.springerlink.com/content/1738-494x
DOI 10.1007/s12206-009-0201-2

Development of rapid mixing fuel nozzle for premixed combustion †

Katsuki Masashi[1], Chung Jin-Do[1], Kim Jang-Woo[1,*], Hwang Seung-Min[1], Kim Seung-Mo[2] and Ahn Chul-Ju[3]

[1]*Hoseo University, 185 Sechul-ri, Baebang-myun, Asan, Chungnam, 336-795, Korea*
[2]*Pusan Clean Coal Center, Pusan National University San 30, Jangjeon-Dong, Geumjeong-Gu, Busan, 609-735, Korea*
[3]*Osaka University, 2-1 Yamada-oka, Suita, Osaka 565-0871, Japan*

(Manuscript Received October 22, 2007; Revised January 7, 2009; Accepted February 3, 2009)

Abstract

Combustion in high-preheat and low oxygen concentration atmosphere is one of the attractive measures to reduce nitric oxide emission as well as greenhouse gases from combustion devices, and it is expected to be a key technology for the industrial applications in heating devices and furnaces. Before proceeding to the practical applications, we need to elucidate combustion characteristics of non-premixed and premixed flames in high-preheat and low oxygen concentration conditions from scientific point of view. For the purpose, we have developed a special mixing nozzle to create a homogeneous mixture of fuel and air by rapid mixing, and applied this rapid-mixing nozzle to a Bunsen-type burner to observe combustion characteristics of the rapid-mixture. As a result, the combustion of rapid-mixture exhibited the same flame structure and combustion characteristics as the perfectly prepared premixed flame, even though the mixing time of the rapid-mixing nozzle was extremely short as a few milliseconds. Therefore, the rapid-mixing nozzle in this paper can be used to create preheated premixed flames as far as the mixing time is shorter than the ignition delay time of the fuel.

Keywords: Burner; Fuel nozzle; Mixing; Premixed combustion; Premixed flame; Rapid mixer

1. Introduction

One of the recent attractive technologies in combustion industry is "*High Temperature Air Combustion* (HiTAC)", in which high performance as well as extremely low nitric oxide emission can be achieved using the highly preheated and diluted air produced by a heat regenerator [1]. The specific feature of HiTAC is that the highly preheated air mixes with burnt products in the furnace before it reacts with the fuel issued separately into the furnace, and it has been held that combustion of low Damkohler number takes place in HiTAC due to the enhanced mixing and prolonged reaction-time in low oxygen concentration condition resulting in the "Well-Stirred Reaction" regime [2]. The database on combustion characteristics and flame structure in low oxygen concentration atmosphere has not been collected in the past, particularly in high temperature range near auto-ignition temperature of the fuel, and several basic researches on HiTAC have been carried out recently paying an attention on the fine-structure of flames [3-9]. As a result, new knowledge is available on "non-premixed combustion" of HiTAC. However, the other extreme would be "high-preheat premixed combustion", as the flame structure may change depending on the local Damkohler number. Therefore, we believe that further study on high preheat premixed combustion is necessary to elucidate and understand HiTAC before we apply HiTAC to practical combustion devices and systems.

† This paper was recommended for publication in revised form by Associate Editor Ohchae Kwon
*Corresponding author. Tel.: +82 41 540 5925, Fax.: +82 41 520 5929
E-mail address: jwkim@ hoseo.edu

Experimental burner for high preheat premixed combustion was not available in the past, particularly for the temperature range of auto-ignition temperature of the fuel used due to flash-back or auto-ignition in the upstream mixture supply line. In order to produce a preheated air stream of 1000 K, some heating methods, such as an electric heater or a pebble heater, are now available. Therefore, if uniform mixture of fuel and oxidizer is formed within a very short duration just before being issued from the nozzle exit, actually shorter than the ignition-delay time of the fuel, we can produce high preheat premixed flames. What we need to precede a further step on HiTAC research will be the development of rapid-mixing nozzle making sure of "high-preheat premixed combustion".

The objective of the present paper is to describe the development of a specially designed mixing nozzle called rapid-mixer of fuel and air to perform turbulent premixed combustion. Practically, we examine whether the inhomogeneity of mixing or fine-scale concentration fluctuations still remains in the reactants stream. From the combustion engineering point of view, we are going to observe the compatibility of the mixture produced by rapid-mixer and the perfectly prepared homogeneous mixture by comparing combustion characteristics of the two mixtures.

2. Numerical analysis of rapid mixer

2.1 Design of experimental burner and geometry of rapid-mixer

We need some idea in designing new combustion rig to observe high-preheat premixed flame. The critical design requirement of the burner is the flow rate capacity of the air-heating device and its operating temperature. Actually, we selected an air-heater, commercially available, working over 1073 K, and the flow rate ranges 50-150 L/min. To reduce the heat loss from the heated air supply line, we adopted a ceramic insulated stainless supply tube, inner diameter of which was 13 mm. Since the ratio of volumetric flow rate of air to fuel is usually large in generating a combustible mixture, we adopted co-axial arrangement of fuel tube placed at the central axis, the outer diameter of which was 6 mm. The estimated Reynolds number based on the annular slit ranges 1,800-5,400 at room temperature.

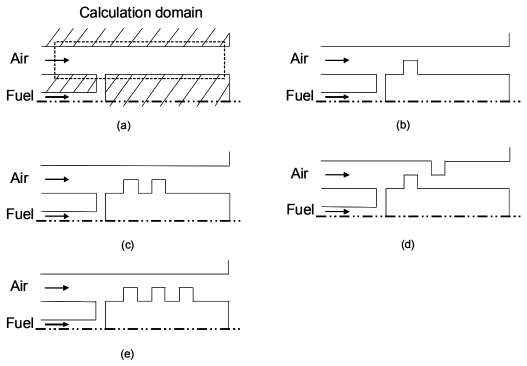

Fig. 1. Calculation domain and geometries of mixer.

In order to mix small flow rate of fuel into the main air flow, the lateral injection of fuel jets may be the most preferable measure as far as we do not use any powered mixing devices. Since allowable mixing time should be shorter than the auto-ignition delay time of the fuel, the twelve lateral fuel injection holes were aligned circumferentially in the cross-section of 42 mm upstream from the nozzle exit, taking the typical ignition delay time in compression ignition engines into consideration.

Under the condition of constant fuel flow rate, the combination of injection holes area and injection velocity may play significant influence on the cross-sectional uniformity of mixture at the mixing-nozzle exit, and the mixing baffles are expected to enhance the mixing during a short pass-time. Therefore, we carried out CFD prediction searching the preferable geometry of the rapid-mixing nozzle.

Fig. 1(a) shows the 50 mm calculation domain of CFD. The outer and inner diameter of the annular air flow channel is 13 mm and 6 mm, respectively. Fig. 1(b) through (e) show the cases with mixing baffles changing their number or orientation, which will be discussed later.

2.2 Mathematical model

In order to see the flow and mixing in the rapid-mixer, numerical simulations were carried out by changing design factors and geometry of rapid-mixers already shown in Fig. 1.

The time-averaged governing equations for steady turbulent flows are written in the following general form,

$$\frac{\partial}{\partial x_j}(\rho \bar{u}_i \phi) = \frac{\partial}{\partial x_j}\left(\Gamma \frac{\partial \phi}{\partial x_j}\right) + S_\phi \quad (1)$$

where, the dependent variable ϕ stands for mass, 1, velocity component in Cartesian coordinates, $\bar{u}_i$, scalar, $\bar{g}$, scalar fluctuation intensity, , turbulence kinetic energy, k, and dissipation rate, ε. The mixture fraction is one of the scalars and is expressed as follows.

$$f = (m_f - m_{f,a})/(m_{f,b} - m_{f,a}),$$
$$\bar{f} = (\overline{m_f} - m_{f,a})/(m_{f,b} - m_{f,a}) \quad (2)$$

Although the definition of fluctuation intensity of mixture fraction, $\bar{g}$, is given by the following equation, actual values are calculated directly by solving the governing equation of the general form,

$$\bar{g} = \overline{(f - \bar{f})^2} \quad (3)$$

where, over-bar is the time-averaged value, m_f is mass fraction of fuel, and the subscript ***a*** and ***b*** denote the values in air and fuel stream, respectively [10]. The dependent variable of each governing equation and corresponding model constants are tabulated in Table 1 and 2.

Turbulence model used was RNG $k-\varepsilon$. Calculation domain of 50mm x 3.5mm x 30degree of fan-shape sector was divided into 100 x 7 x 5 calculation grids, and the discritized governing equations were solved by SIMPLE algorithm [11] in FLUENT software.

2.3 *Numerical results and influencing factors of rapid mixing*

Fig. 2 shows the influence of fuel injection velocity as well as the momentum of fuel jet on the uniformity of mixture fraction at the exit of rapid-mixer. Deep penetration of lateral fuel jet is not predicted in case of low injection velocity. When fuel injection velocity is increased keeping the area of fuel injection holes constant, hence the increased fuel flow rate, the peak position in radial distribution of mixture fraction moves outward. Although the radial profile is not yet uniform, injected fuel has reached the peripheral part of the main flow. It means that the momentum of fuel injection should be high to some extent to mix the lateral jet with the main air flow, and some additional

Table 1. Dependent variable and corresponding terms in general form Eq. (1).

ϕ	Γ_ϕ	S_ϕ
1	0	0
$\bar{u}_i$	$\mu+\mu_t$	$\frac{\partial}{\partial x_j}\left((\mu+\mu_t)\frac{\partial \bar{u}_j}{\partial x_i}\right)-\frac{\partial}{\partial x_i}P$
k	$\mu+\frac{\mu_t}{\sigma_k}$	$\mu_t(P+P_B)-\bar{\rho}\varepsilon-\frac{2}{3}\left(\mu_t\frac{\partial \bar{u}_i}{\partial x_i}+\rho k\right)\frac{\partial \bar{u}_i}{\partial x_i}$
ε	$\mu+\frac{\mu_t}{\sigma_\varepsilon}$	$C_{\varepsilon 1}\frac{\varepsilon}{k}\left(\mu_t P-\frac{2}{3}\left(\mu_t\frac{\partial \bar{u}_i}{\partial x_i}+\rho k\right)\frac{\partial \bar{u}_i}{\partial x_i}\right)+C_{\varepsilon 3}\frac{\varepsilon}{k}\mu_t P_B$ $-C_{\varepsilon 2}\bar{\rho}\frac{\varepsilon^2}{k}+C_{\varepsilon 4}\bar{\rho}\varepsilon\frac{\partial \bar{u}_i}{\partial x_i}-\frac{C_\mu\eta^3(1-\eta/\eta_0)}{1+\beta\eta^3}\frac{\bar{\rho}\varepsilon^2}{k}$
$\bar{f}$	$\mu+\frac{\mu_t}{\sigma_m}$	0
$\bar{g}$	$\mu+\frac{\mu_t}{\sigma_g}$	$C_{g1}\left[(\mu+\frac{\mu_t}{\sigma_g})(\frac{\partial \bar{f}}{\partial x_i})^2\right]-C_{g2}\bar{\rho}\frac{\varepsilon}{k}\bar{g}$

Table 2. Turbulence and mixing model constants.

C_μ	σ_k	σ_ε	σ_m	σ_g	$C_{\varepsilon 1}$	$C_{\varepsilon 2}$	$C_{\varepsilon 3}$	$C_{\varepsilon 4}$	η_0	β	C_{g1}	C_{g2}
0.085	0.719	0.719	0.9	0.9	1.42	1.68	1.42	-0.387	4.38	0.012	2.8	2.0

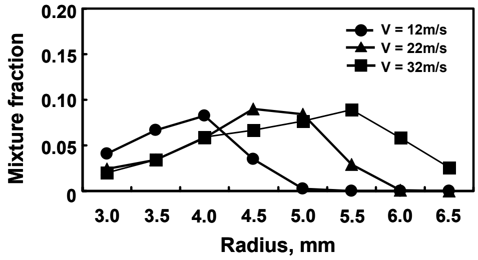

Fig. 2. Influence of fuel injection velocity with constant injection hole area (Equivalent diameter = 0.5 mm).

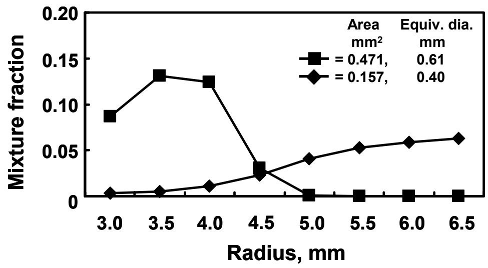

Fig. 3. Influence of fuel injection hole area with constant flow rate.

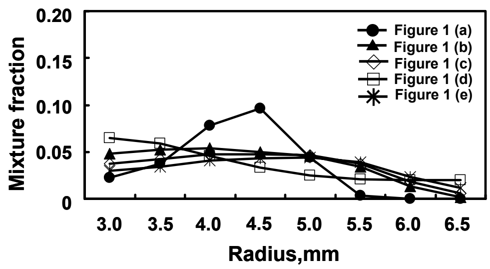

Fig. 4. Influence of mixing baffle.

enhancement of mixing in the mixing-nozzle will probably bring about the uniformity at the exit of the mixer.

To verify the effects stated above, we changed the opening area of fuel injection holes keeping the fuel flow rate constant. In Fig. 3, the low velocity fuel jet from wide injection hole produced the profile of mixture fraction partial to the inner side of the main flow, and the more uniform distribution is predicted in case of high velocity fuel jet from small injection hole. Namely, in order to mix a small lateral jet with a large main flow, the momentum of the small jet should be high so that the fuel jet penetrates deeply into the main flow. Accordingly, we selected the fuel injection hole diameter of 0.5 mm with injection velocity of 27.3 m/s to carry out the present experiments taking account of further effects of mixing baffles.

Fig. 4 shows the effect of baffles on the mixing processes. Since a baffle bends the streamline and generates a recirculation flow behind it, mixing processes are enhanced by the baffle. We have compared the influence of mixing baffle by adding baffles as illustrated in Fig. 1. The radial mixture faction profiles at the exit of rapid-mixer are seen to be more uniform as the number of baffles increases. When the orientation of baffles is changed alternatively, the resulting radial mixture fraction profile is affected by the winding motion of the main flow forced by the orientation of baffles.

The more baffles, the better mixing we can expect. At the same time, however, the total pressure loss in the supply line will increase. The increase of total pressure loss from two-staged to three-staged baffles was predicted to be 20 Pa. Since machining process on ceramic insulation tube is not easy, we decided to adopt multi-staged mixing baffles on the inner tube, and concluded that case (e) of Fig. 1 is the best to generate the preferable mixture distribution among the cases examined.

We can apply our present idea to large scale burners, however, the geometries shown here is not always a design standard, because the most predominant design factor of well mixing of a small lateral jet into the main flow was found to be the momentum ratio of the two streams. In that sense, physical properties, such as density and diffusivity, of the miner fluid may also be important factors to affect on the momentum ratio, even if we keep Reynolds number constant.

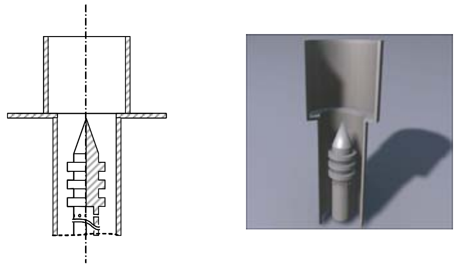

Fig. 5. Rapid-mixer and burner configuration.

3. Burner and fuel mixing nozzle

3.1 Experimental apparatus

Taking into consideration of the results obtained in the previous section, we designed a rapid-mixing nozzle for premixed combustion expecting to create homogeneous mixture in several milliseconds. Figure 5 shows the details of the rapid-mixer. A ceramic tube of 13 mm inner diameter is used for the insulation of air supply tube and the lateral fuel jets from fuel tube of 6 mm outer diameter are injected through 12 holes of 0.5 mm diameter to give large lateral momentum in the cross-section of 42 mm upstream from the nozzle exit. Three staged mixing baffles of the same orientation are placed downstream of the fuel jets and the tip of mixing-nozzle is sharpened to expand the mixture flow into the burner, and the sudden expansion step of the mixer works as a flame stabilizer of the burner. The coordinate of measuring positions are set as in the figure. The nominal pass-time of mixture from fuel nozzle to the mixer exit was estimated 4.5 ms, when the flow rate of air was the minimum among the experimental conditions.

3.2 Experimental procedures

Fig. 6 shows the experimental set-up. In case of premixed combustion, homogeneous mixture is prepared in the mixing chamber settled far upstream from the burner by introducing compressed combustion air and city gas. By switching the three-way valve, fuel is introduced directly to the rapid-mixing nozzle placed in the center of burner when we want to operate with rapid-mixture.

In preliminary experiments, flow rate of mixture was varied between 55 L/min and 110 L/min taking the air flow rate of future experiments. The corresponding Reynolds number was estimated as 2000 and 4000, respectively, based on the flow velocity and the width of the annular flow channel. We de-

Table 3. Experimental conditions.

	Q_{air}, L/min	t_{mix}, ms	u', m/s	ϕ
Premixed (PP)	55	–	1.15	0.7
Rapid-mixed (RM)	55	4.5	1.15	0.7

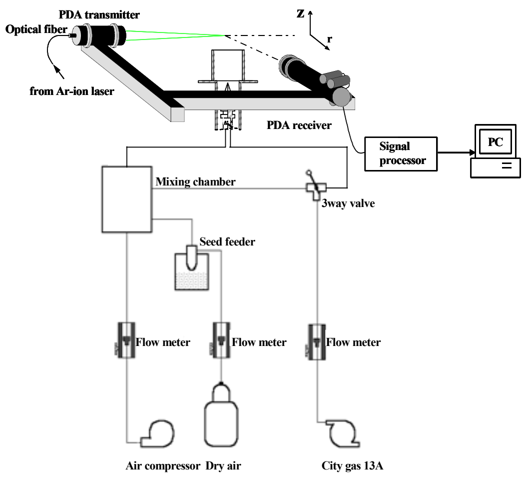

Fig. 6. Experimental set-up.

cided to keep the equivalence ratio constant of 0.7, because the mixing processes would not be influenced by the equivalence ratio. The value was determined to keep the estimated temperature lower than the durable limit of the fine-thermocouple used in later experiments. The experimental conditions carried out are tabulated in Table 3.

The flow and turbulent characteristics were measured by laser Doppler velocimetry (LDV). Laser source used was Ar^+ CW laser (NEC, Model GLG-3462) and the receiving optics was DANTEC (Model 57X10). The micro-silica balloon of 2.7 μm mean diameter was used as the tracer of the flow and mixed with combustion air as shown in Fig. 6. The detected LDV signal were processed by an LDV signal processor (DANTEC, Model 58N10) and recorded by a personal computer. We deduced the mean flow velocity, turbulent intensity and integral scale of turbulence from 32768 LDV data obtained by the acquisition rate of 5 to 60 kHz. The integral scale was calculated by the slot-method using time series intermittent velocity signals [12, 13].

Gaseous species were sampled through a water-cooled probe and analyzed by a gas chromatograph and a NOx analyzer, and the obtained concentrations are time-averaged values,

Temperature was measured using a silica coated R-type thermocouple of 25 μm wire diameter. Voltage signal of the thermocouple was amplified by a pre-amplifier, passing through a low-pass filter of 5 kHz and converted by an A/D converter, and then recorded by a PC. The recorded signals were compensated for the thermal inertia due to heat capacity of the welded bead of the couple and its radiation heat loss. Though the frequency limit of compensated thermocouple was estimated to be around 10 kHz, no signals higher than 2.5 kHz were observed in actual flames. So, the frequency limit of compensated thermocouple system was thought to be about 2.5 kHz [14].

Detection of ion-current in flames is a useful measure to examine local reaction-zone structures of turbulent premixed flames, and we can evaluate spatial scale of existence of chemical reaction [15]. The sensing wire of electrostatic Langmiur probe was a Pt-Rh13 wire of 0.1 mm and 0.5 mm long, and kept -18V relative to the burner and the earth. The detected current signals were transformed into voltage signals by I-V converter (NF Electronic LI-76) and amplified by a V-V amplifier and filtered by a low pass filter (cut off frequency 2.5 kHz), then recorded by a PC through an A/D converter (sampling time 20 μs). The characteristic time scale of existence of chemical reaction was obtained from auto-correlation coefficient.

4. Experimental results and discussion

4.1 Direct photography and fuel concentration in reactants

Fig. 7 shows the direct photographs of perfect premixed (**PP**) flame and rapid-mixed (**RM**) flame formed on the Bunsen-type turbulent burner, which were taken with same exposure time and magnification for the both cases. The shape, length and color of the rapid-mixed flame look similar to the perfect premixed flame. If mixing between fuel and air was imperfect and some fluctuations in concentration retained, the total flame length would be longer for rapid-mixed flame and local yellow flickering of flame would appear. It was difficult to point out the differences between the two images, which may suggests us that the mixing by the rapid-mixer is almost perfect. As was suggested by numerical prediction, mixing in higher velocity cases, though not shown here, looked better judging from the shape, length and color of the flames. Therefore, we will examine the

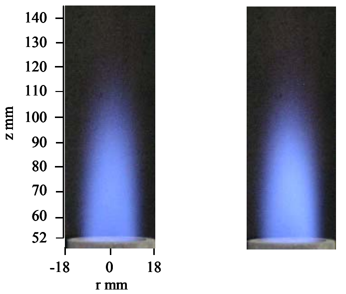

(a) Premixed flame (PP) (b) Rapid-mixed flame (RM)

Fig. 7. Direct photograph of flames.

combustion characteristics of lower velocity cases by detailed measurements.

We measured the fuel concentration in the reactant stream to examine the uniformity of fuel distribution in the burner by analyzing sampled mixtures. As a result, the time-averaged fuel concentration showed the same value as of the perfect mixture. Since the measured concentrations obtained by a gas chromatograph are time-averaged values, there remains a doubt that the existence of concentration fluctuations, in other words, small-scale inhomogeneity, which may influence on combustion reaction. Accordingly, we carried out the observation of fine structure of turbulent flames formed in the rapid-mixture using flame diagnosis, and compared the data with those of perfect mixture.

4.2 Flow field and turbulence characteristics

The distributions of axial velocity, turbulence intensity and integral length scale of turbulence are shown in Fig. 8. The time-averaged axial velocity takes almost uniform value along the axis. The turbu lence intensity does not show a noticeable change from upstream to downstream as is like the time-averaged axial velocity. Since the actual turbulence intensity is around 1 m/s, the flame seems to be dominated by relatively weak turbulence. The integral scale of turbulence starts from about 3 mm at the mixer exit to grow gradually and suddenly to be 20 mm downstream toward the flame tip. When we compare the distributions of axial velocity, turbulence intensity and integral length scale of turbulence for the perfect premixed mixture with those for the rapid-mixture, the measured quantities are resemble each other, and we can say that the equality of turbulence characteristics in both flames is quite high. Accordingly, turbulence characteristics defined mostly by the geometry of mixer, mixing baffles in particular, dominate the turbulence field of the burner, and the influence of cross-flow jets of fuel is not significant.

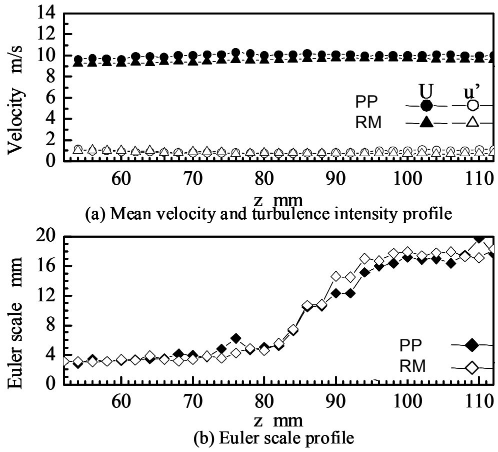

Fig. 8. Flow and turbulence properties.

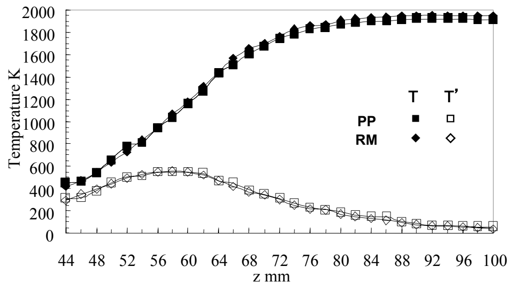

Fig. 9. Mean temperature and fluctuation intensity.

4.3 Temperature and flame structure

The distributions of mean temperature and ***rms*** of temperature fluctuations along the axis are shown in Fig. 9. The profile of mean temperature rises up around *Z*=44 mm and reaches the maximum around *Z*=90 mm, and ***rms*** of fluctuations takes the maximum value around *Z*=60 mm and declines gradually. The gradual decay in the downstream side of the maximum value of mean temperature and small temperature fluctuations means that most of fuel is burned until the maximum mean temperature that is taken as the nominal flame tip. Those features stated above are similarly observed in either flame run by perfect premixed mixture and by rapid-mixture.

Fig. 10 shows probability density distributions of temperature fluctuations for both perfect premixed flame and rapid-mixture flame. The shape of distribu-

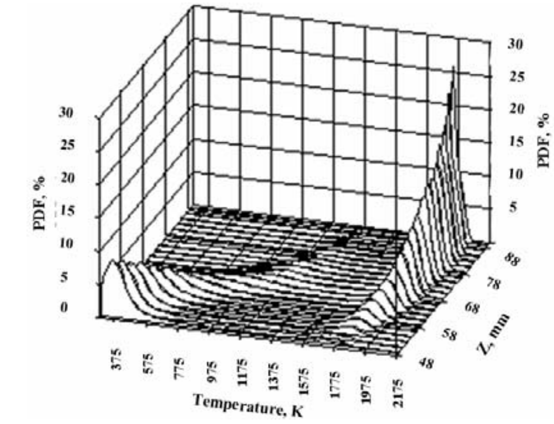

(a) Premixed flame

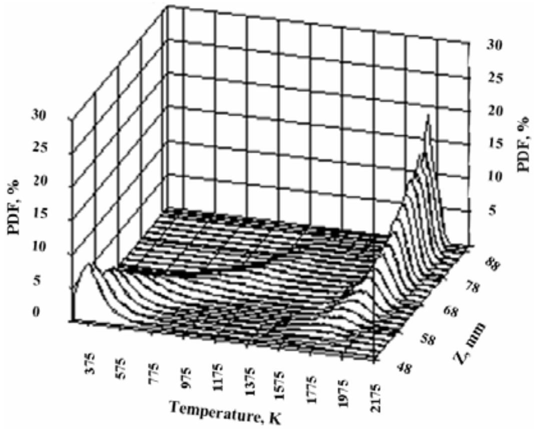

(b) Rapid-mixed flame

Fig. 10. Probability density distributions of fluctuating temperatures.

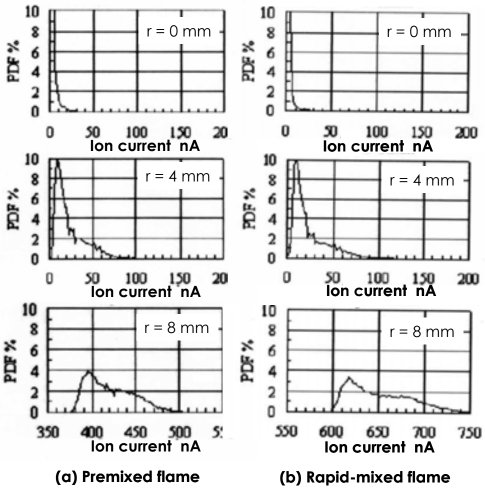

Fig. 11. Probability density distributions of fluctuating ion currents.

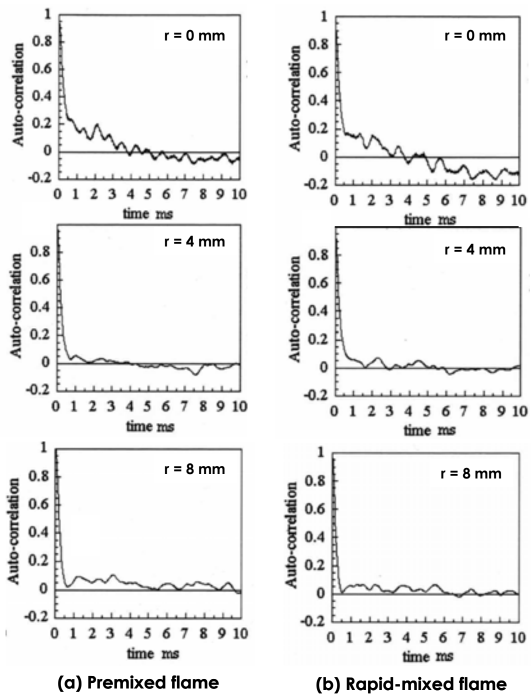

Fig. 12. Auto-correlation coefficients of ion current signals.

tion changes from the unburned state where high probability appears at low temperature of unburned mixture to the final burned state where high probability stands at high temperature of burned gas through the intermediate stages where bi-modal distributions including intermediate temperatures to some extent depending on the progress of combustion reaction[16]. Adding to the fact above, the same features in probability density distribution of temperature distributions were observed for other experimental conditions not shown here.

Temperature level for fully burned gas varies depending on the local equivalence ratio of mixture. Then, if there are any fuel concentration fluctuations in the unburned mixture, we will have a widened peak at high temperature side in the probability density distribution. Since the width of high temperature peaks for the rapid-mixture flame looks almost the same for the perfect premixed flame, we can conclude that the rapid-mixture flames have the similar thermal structures as the perfect premixed flames.

4.4 Ion-current in flames

Judging from the flow velocity and turbulence

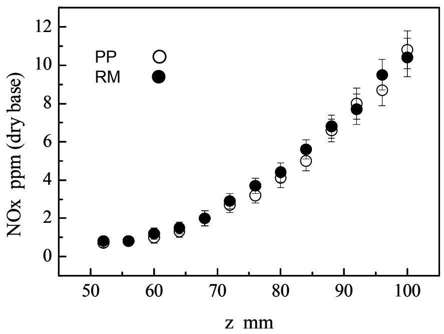

Fig. 13. Distribution of nitric oxide formed in flames.

characteristics discussed in the previous section, we consider the fine structure of turbulent premixed flames we are interested here is classified to be the regime of “wrinkled laminar flame”. Therefore, the measured ion-current signals correspond to passage of thin reaction zone, that is a flamelet, being carried by turbulent motion of fluids.

The typical examples of probability density distributions of ion-current signals and auto-correlation coefficients are shown in Fig. 11 and Fig. 12, respectively. Characteristics of ion-current for the perfect-premixed flame and for the rapid-mixed
flame seem to be almost identical each other.

Based on those facts, we conclude that the structure of reaction zone and the spatial density of reaction are almost the same for both flames. Accordingly, mixing enhancement by the rapid- mixer can create almost perfect mixture within a short passing-time.

4.5 Nitric oxide emission

We measured nitric oxide emission of the two types of flame we had been observing. The gases in flames were sampled through a water-cooled probe and analyzed by a NOx analyzer. The values of concentration are as measured. The change of nitric oxide concentration along the burner axis is shown in Fig. 13. From upstream to downstream, nitric oxide concentration increases with the progress of combustion, and the almost perfect coincidence of distributions for the perfect premixed flame and the rapid-mixture flame was obtained. It has been held that the formation rate of nitric oxide in flames strongly depends on temperature as well as on residence time particularly in high temperatures over 1800 K. Therefore, the agreement of nitric oxide concentration in the two flames means that combustion characteristics and thermal structures of the perfect premixed flame and the rapid-mixture flame are considered to be compatible from the stand point of practical combustion engineering.

5. Concluding remarks

We have successfully developed a rapid-mixer to create homogeneous mixture of fuel and air using CFD design procedure, and exploited the combustion characteristics and flame structure of the flame formed by the rapid-mixture comparing with those of the perfect premixed flame.

We measured the flow and turbulence characteristics, thermal structure and chemical structure as well as nitric oxide emission of the rapid-mixture flames, and compared them with those of perfect premixed flames. The mixture created by the rapid-mixer showed similar combustion characteristics to the perfect premixed mixture in spite of the short pass-time through the rapid-mixer. Accordingly, we believe that the rapid-mixture flames described in this paper were classified premixed flames from the practical combustion engineering point of view.

The facts shown above are not new scientific findings by themselves but of hopeful new experimental measure to enable us to pursue future scientific observation on premixed combustion in extremely high preheat circumstances. It also gives us a basic concept in designing practical combustion devices free from flash-back.

References

[1] H. Tsuji, et al., High Temperature Air Combustion, CRC Press, (2002).

[2] M. Katsuki and T. Hasegawa, The Science and Technology of Combustion in Highly Preheated Air, Proc. Combust. Inst. 27 (1998) 3135-3146.

[3] P. R. Medwell, et al., Imaging of diluted turbulent ethylene flames stabilized on a Jet in Hot Coflow (JHC) burner, Combustion and Flame 152 (2008) 100-113.

[4] T. Yokomori, et al., Electrostatic probe measurement in an industrial furnace for high-temperature air conditions, Combustion and Flame 150 (2007) 369-379.

[5] C. Galletti, et al., Numerical and experimental investigation of a mild combustion burner, Combustion and Flame, 151 (2007) 649-664.

[6] P. R. Medwell, et al., Simultaneous imaging of OH, formaldehyde, and temperature of turbulent non-premixed jet flames in a heated and diluted coflow, Combustion and Flame 148 (2007) 48-61.
[7] B. B. Dally, et al., Effect of fuel mixture on moderate and intense low oxygen dilution combustion, Combustion and Flame 137 (2004) 418-431.
[8] H. Kobayashi, et al., Effects of Turbulence on Flame Structure and NOx Emission of Turbulent Jet Non-premixed flames in High-Temperature Air Combustion, JSME Int. J. 48B-2 (2005) 286-292.
[9] J. H. Kwark, et al., Combustion Characteristics of a Turbulent Non-Premixed Flame using High Preheated Air, KSME Trans. 27 (5) (2003) 561-568.
[10] E. E. Khalil, et al., The Calculation of Local Flow Properties in Two-Dimensional Furnaces, Int. J. Heat Mass Transfer 18 (1975) 775-791.
[11] S. V. Patankar, Numerical Heat Transfer and Fluid Flow, McGraw-Hill, (1980).
[12] H. R. E. Van Maanen, et al., Improved Estimator for the Slotted Autocorrelation Function of Randomly Sampled LDA Data, Meas. Sci. Technol. 10 (1999) L4-L7.
[13] L. H. Benedict, et al., Estimation of Turbulent Velocity Spectra from Laser Doppler Data, Meas. Sci. Technol. 11 (2000) 1089-1104.
[14] M. Katsuki, et al., An Improved Thermocouple Technique for Measurement of Fluctuating Temperatures in Flames, Combustion and Flame 67 (1987) 27-36.
[15] J. Furukawa, et al., Local Reaction Zone Configuration of High Intensity Turbulent Premixed Flames, Combust. Sci. Tech. 90 (1993) 267-280.
[16] M. Katsuki, et al., Local Flame Structure and its Influence on Mixing Processes in Turbulent Premixed, Combustion and Flame 82 (1990) 93-105.

Masashi Katsuki received his B.E. degree in Mechanical Engineering from Osaka University, Japan, in 1965. He received his Dr. Eng. from O. U. in 1985. Dr. Katsuki is currently a Visiting Professor at the Department of Environmental Engineering at Hoseo University in Chungnam, Korea. He was a Vice President of the Japan Society of Mechanical Engineers. Dr. Katsuki's research interests include combustion, computational thermo-fluid dynamics, and molecular dynamics.

Jin-Do Chung received his B. S., M.S. and Ph.D. degrees in Mechanical Engineering from Chungnam University, Korea in 1983, 1985 and 1990. He then received another Ph.D. in Environmental Engineering from Kanazawa University, Japan in 1996. After that he worked as Post-doc researcher for 1,6 year at KIMM and Senior researcher for 6years at KEPCO Research Center. Dr. Chung is currently a Professor at the Department of Environmental Engineering at Hoseo University in Asan, Korea. Dr. Chung's research interests include thermal-fluid and environmental engineering.

Jang-Woo Kim received his B. S. degree in Mechanical Engineering from Chungnam University, Korea, in 1990. He then received his M. S. and Ph. D. degrees from Kyushu University, Japan in 1994 and 1998, respectively. Dr. Kim is currently a Professor at the School of Display Engineering at Hoseo University in Asan, Korea. Dr. Kim's research interests include CFD, aerodynamics, and display equipment technology.

Seung-Min Hwang received the Ph.D. degree in Mechanical Engineering at Osaka University in 2005. After that he worked as visiting researcher for 3 years at CRIEPI (central research institute of electric power industry) and Osaka University in Japan. He is currently a Professor at the Graduate School of Venture at Hoseo University in Korea. His major research is thermal-fluid, energy issue and environment.

Seung-Mo Kim received his Ph. D. degrees in Mechanical engineering from Osaka University, Japan, in 2004. Dr. Kim is currently a research Professor at Pusan Clean Coal Center at Pusan National University in Pusan, South Korea. Dr. Kim's research interests include coal combustion, oxy-fuel combustion, coal gasification, coal de-watering, power generation plant system and energy issues.

Chul-Ju Ahn received his B.S. degree in Mechanical Engineering from Hanyang University, Korea, in 1998. He then received his M.S. and Ph.D. degrees from Osaka University, Japan, in 2001 and 2006, respectively. Dr. Ahn is currently a Senior Research Engineer at Samsung Techwin CO. LTD. in Changwon, Korea. Dr. Ahn's research interests include gas turbine engine, biomass gasification, and power system.